Title

Proceedings of the Second Symposium on Ion Sources and Formation of Ion Beams

Authors

Kulygin, V M
Panassenkov, A A
Semashko, N N
et al.

Publication Date

1974-10-01

LBL-3399 Suppl.

SUPPLEMENT

Proceedings of the

Second Symposium on Ion Sources and

Formation of Ion Beams

Berkeley, California

22-25 October 1974

DISCLAIMER

STUDY OF THE OSCILLATIONS IN REFLEX-ARC ION SOURCE PLASMA AND ITS INFLUENCE ON EXTRACTED BEAM TRANSVERSAL DISPERSEDNESS

V.M.Kulygin
I.V.Kurchatov Institute of Atomic Energy
Moscow , USSR

Abstract

Ion source reflex-arc plasma oscillations are investigated.It is found that frequencies of most intensive oscillations in discharge plasma take place in the diapason from 50 kc to 1Mc.These oscillations are caused by rotating disturbances and may be divided into two kinds.The first kind of oscillations take place if neutral hydrogen pressure in discharge chamber is relativly small.According to its main characteristics these oscillations can be identified as a drift-dissipative instability, modified by rotation in crossed electric and magnetic fields.The second kind of oscillations take place when charged particle-neutral collision frequencies become quite big.The most probable reason of these oscillations - instability, rising from difference between ion and electron "friction" against a neutral gas.The main working pressure diapason where ion beam was extracted, was that, where the first kind of oscillations took place.In this work an influence of these oscillations on ion beam transversal dispersedness is studied.Measurements demonstrate increasing of beam dispersedness when discharge oscillations amplitude is increased.

STUDY OF THE OSCILLATIONS

The discharge chamber was 10cm long and 1cm transverse. Hydrogen pressure could be varied from $1.4 \cdot 10^{-3}$ up to $2.5 \cdot 10^{-2}$ tor. Probes were placed along and around the chamber; currents from these probes were studied by means of oscilloscopes and a spectrum analyser, which worked in the frequency diapason from 30 kc to 30Mc .

Frequencies of most intensive oscillations in discharge plasma took place in diapason from 50 kc to 1 mc. Probes signals phase shift mesuruements allowed us to determine that at least first harmonics of all investigated probe signal oscillations were caused by rotating disturbances with $k \to 0$. This rotation had the same direction that the plasma drift in crossed fields, if we took into account negativ potencial on the reflex-arc axis [1] [2]. Mentiond oscillations may be divided into two kinds. Fig.1 shows that when external magnetic field was equal to 1000 gauss,the first kind of oscillations took place if neutral hydrogen pressure was less then $3 \cdot 10^{-3}$; if this pressure was $> 3 \cdot 10^{-3}$, second kind of oscillations took place. The second kind oscillations amplitude rose with pressure increasing up to $1 \cdot 10^{-2}$, then became decreasing. When neutral gas pressure was 1.5 - $2.5 \cdot 10^{-2}$tor , all oscillations were disappered.

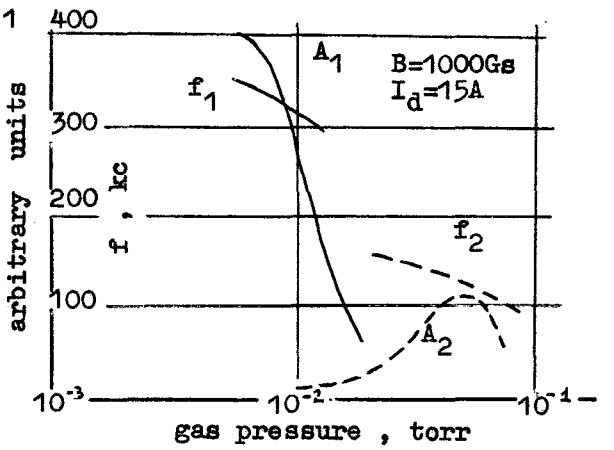

Fig.1
Amplitudes and frequencies of oscillations the first and the second kinds as a functions of gas pressure.

Basic characteristics of oscillations are illustrated by figures. All data are given for the first harmonics (for the first azimuth mode of rotating disturbance)

1. Oscillations of the first kind

These oscillations take place on frequencies of some hundred kc(the first harmonic - 200 - 300 kc). Usually there are three harmonics; its frequencies increases with discharge current rising (fig.2). On the same figure one can seethat an oscillations amplitude become sharply large when discharge current approaches value 9-12 A. Character of the first kind os-

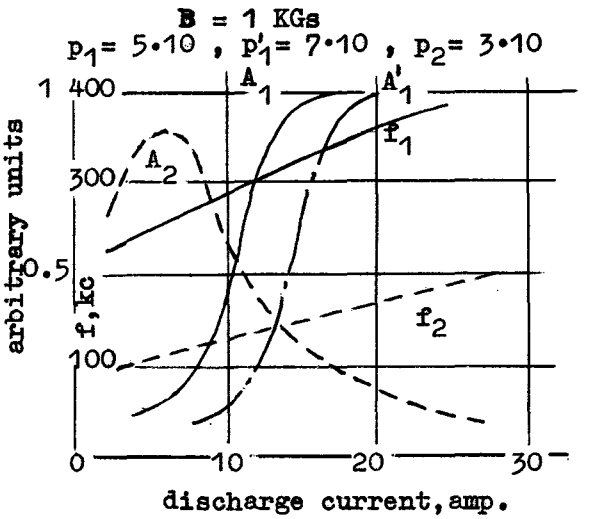

Fig.2.
Amplitudes and frequencies of oscillations of the first and the second kinds as a functions of discharge current.

cillations frequency and amplitude dependence on a magnetic field is shown on fig.3.One can see a threshold above which amplitude sharply increases. The frequancy rises linearly with a magnetic field. One ought to note an influence of this sort of oscillations on external discharge characteristics.Fig.4 gives a dependence of a discharge current and voltage on a magnetic field.If to compare fig.3 and fig.4 , one can see that discharge resistance has a minimum in the point of oscillations amplitude maximum. It looks as if these oscillations make electrones going to anode across a magnetic field.

2. Oscillations of the second kind

These oscillations take place on some lower frequencies (the first harmonic - 50 - 120 kc). From figures one can see that their amplitude has a maximum when a discharge current is eq-

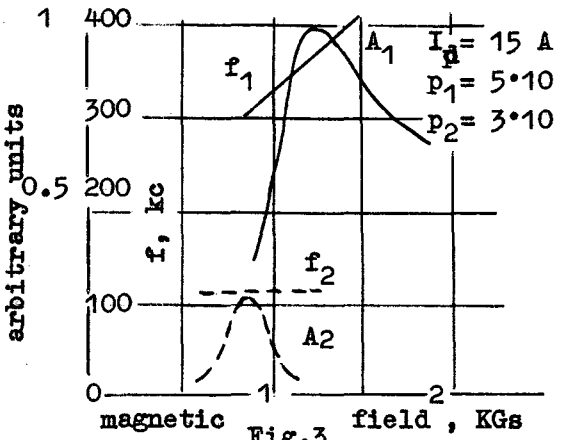

Fig.3
Amplitudes and frequencies of oscillations of the first and the second kinds as a functions of magnetic field.

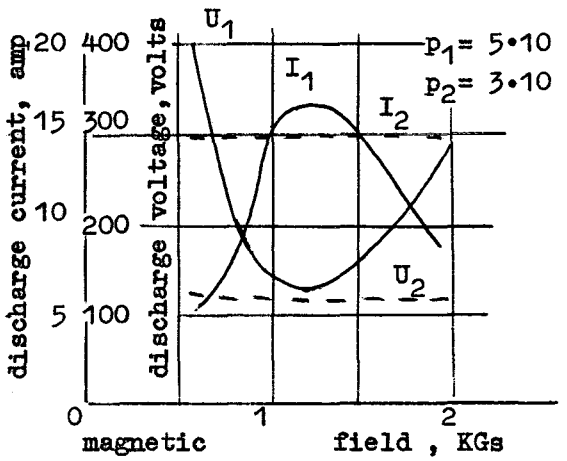

Fig.4
Discharge current and voltage as a functions of magnetic field. 1 - when the first kind oscillations take place ; 2 - the second kind oscillations take place.

ual to some about 5 - 8 A.Their frequency increases monotonously with discharge current increasing (fig.2).Amplitude dependence on magnetic field has more resonant character than that for the first kind, but a frequency is independent on a magnetic field (fig3) External discharge characteristics is practically independent on the second kind oscillations amplitude.

3. Discussion

First of all we ought to pay attention to the fact of all oscillations under consideration disappearence when neutral gas pressure exceeds certain value. This value changes with changing of a magnetic field magnitude. It was found that all oscillations was

disappeared when ion-neutral collision frequency approached to ion cyclotron frequency. Therefore, it was interesting to drow a curve of oscillations amplitude dependence from ratio ν_{in}/ω_{Bi}. Such a curve is drown on fig.5. We can

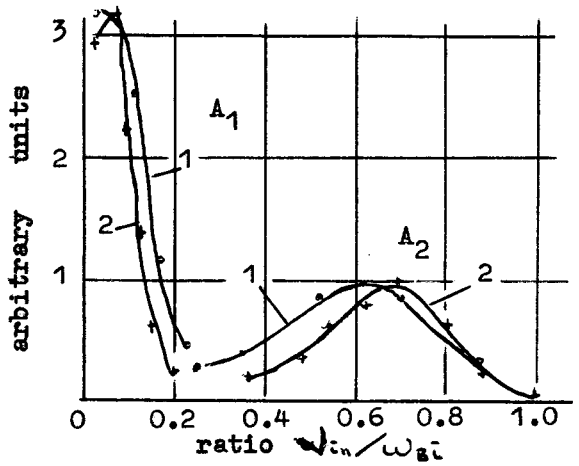

Fig.5.
Oscillations amplitude dependence from ratio ν_{in}/ω_{Bi}. 1 - by pressure variation; 2 - by variation of magnetic field.

see that oscillations of the first and the second kind were developed when $\eta \equiv \nu_{in}/\omega_{Bi} < 1$. The first kind oscillations took place only when $\eta \ll 1$. They were damped by collisions frequency increasing, or magnetic field decreasing. Second kind oscillations took place when ion-neutral collisions were quit e frequent ($\eta \lesssim 1$). Frequency diapason, spacial structure of both kinds of oscillations and their developing in region $\eta < 1$ permits us to suggest the drift nature of these oscillations. But, probably, two kinds of oscillations have differ develop mechanisms. So, they must be discussed separately.

a) Oscillations of the first kind - are disturbances which rotates in the direction of crossed fields plasma drift. They develop on frequencies $\omega_k \gtrsim \nu_{in}$. They are stretched along z - axis ($K_\perp \gg K_z$). It is well known that accounting of little frequency collisions and $K_z \ll K_\perp$ (without external radial electric field E_r) gives a developtment of a drift-dissipative instability [3]. Dispertion equation

$$\omega^2 + i\omega(\omega_s + D_e K_z^2 + \nu_{in}) - i\omega_s\omega_* - D_e K_z^2 \nu_{in} = 0 \quad (1)$$

where

$$\omega_* = -k_\varphi \frac{cT_e}{eH} \frac{1}{n}\frac{dn}{dr} \; ; \; \omega_s = \frac{K_z^2}{K_\perp^2} \omega_{Be}\omega_{Bi}\frac{1}{\nu_{en}} \quad (2)$$

ω_{Be}; ω_{Bi} - electron and ion cyclotron frequencies ;
ν_{en}; ν_{in} - electron-neutral and ion-neutral collision frequencies ;
D_e - electron diffusion coefficient.

For our experiments $\omega_s \ll \omega_*$, and in this case

$$\omega_1 = \sqrt{\omega_s \omega_*} \quad (3)$$

According to (2) and (3) a drift-dissipative instability oscillations frequency must rise with increasing of magnetic field. Electric field must cause a Doppler shift of the frequency: $\omega_k = \omega_1 + \omega_E$, where $\omega_E = \frac{1}{R}(cE_z/eB_z)$ (4) Such a drift instability variety may be used for interpretation of our experimental results. Really, an oscillation frequency rising with rising of magnetic field is observed. Then, when ion-neutral collisions become quite frequent, $\nu_{in} \to \gamma \sim \sqrt{\omega_s \omega_*}$, oscillations are strongly damped. Same collisions decrease ω_k by decreasing of ω_E effective value. As increment is dependent from B_z and from density gradient, so critical values of these parameters have to exist. For such values an increment becomes sufficient for to overcome oscillation damping. Certainly, damping rises with ν_{in}. So, critical values must rise with collisions frequency increasing. There is a quality agreement with a presence of a discharge current and magnetic field thresholds shift, demonstrating on figures. Structure of ω_k in eq.(4) is agree with data of fig.1. After the first kind instability becomes damped by collisions, the term ω_1 of eq.(4) disappeares. An oscillation frequency sharply decreases and becomes near ω_E; in the system second kind oscillations developes.

B) Oscillations of the second kind - have quite similar space structure. But they need more neutral gas in the discharge chamber. Frequency of this kind of oscillations $\omega < \nu_{in}$.

Weakly ionized plasma in crossed electric and magnetic fields was investigated by Hoh [4] and Simon [5]. Main results of these papers were agree.

In a plasma, placed into crossed fields, instability caused by difference in electrons and ions frictions against a neutral gas can be excited. The nesessary condition for this exciting is :

$$E_{cr}\frac{\partial v_0}{\partial r} > 0 \quad (7)$$

This condition is always satisfied in a reflex-arc plasma. For rising an os-

cillations amplitude it is nesessary to have the left-hand side of (7) more then some positive value. Oscillation frequency for the first mode of disturbance is

$$\omega_K \approx \frac{1}{R}\frac{E_{02}}{B_0}\left[1+\left(\frac{\nu_{in}}{\omega_{Bi}}\right)^2\right]^{-1} \quad (8)$$

and increment for $\eta < 1$

$$\gamma \approx \eta \left|\frac{e}{m} E_{02} \frac{1}{w} \frac{\partial n}{\partial z}\right|^{1/2} \quad (9)$$

From (8) we can see that frequency must rise with discharge current rising and decrease with gas pressure increasing. From (9) we can see that oscillations have to develop with rising of η and with dencity and potential gradients increasing. But when $\eta \to 1$ the mobility stabilisation become suffisient. Oscillations are damped.

DISPERSEDNESS MEASUREMENTS

In usual conditions of ion sourse operating first kind oscillations were developed. So , we studied their influence on ion energy dispersedness.

The scheme of experiment is given on fig.6. Ions are extracted from a gas discharge plasma and accelerated across a magnetic field. The measuring device is placed on the "grounded" plate of the extracting system. Some part of the ion stream falls on the massive tungsten plate. The rest beam passes by. The tungsten plate has a calibrated aperture which picked out a weak ion jet. The jet space charge is neglectable. A presence of an ion transversal velocity spectrum put the jet to diverge. One can get an information about transversal ion energies by measuring of transversal jet current distribution on a definite distance from the calibrated aperture.

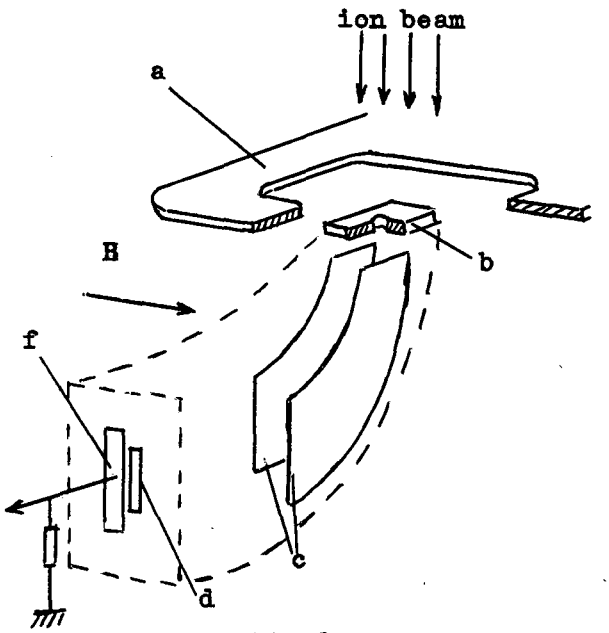

Fig.6
The scheme of dispersedness measurements experiment.
a - the Grounded plate of the extracting system ;
b - the massive tungsten plate ;
c - deflection plates ;
d - the collector slit ;
f - collectir plate .

Measurements were made by such a way : the jet was driven across a narrow collector slit by saw-tooth voltage, supplied to deflection plates. A signal from the collector plate was supplied to a vertical-deflection amplifier of oscilloscope; scanning of the oscilloscope was operated by the same saw-tooth voltage. In result , there was a transversal jet current distribution curve on the oscilloscope screen. This system was calibrated for to get an information about an ion energy distribution directly from the oscilloscope screen.

It was possible to use two deflection systems in turn in this device. One of them could drive the jet along a magnetic field, and another - across.

Two extraction slits were used for to extract ions from a discharge. The first slit was 40 mm along magnetic field and second - 2 mm. Their dimentions across magnetic field were 4 mm. Dispersedness was measured in both directions.

Main results of our measurements are demonstrated on figures 7 - 10 .

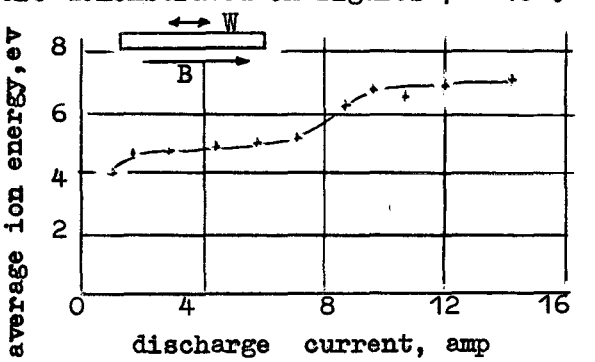

Fig.7
The average transverse ion energy along the magnetic field as a function of a discharge current. Longitudial extraction slit.

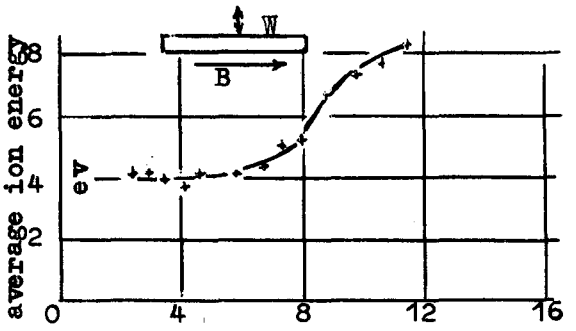

Fig.8

The average transverse ion energy across the magnetic field as a function of a discharge current. Longitudial extraction slit.

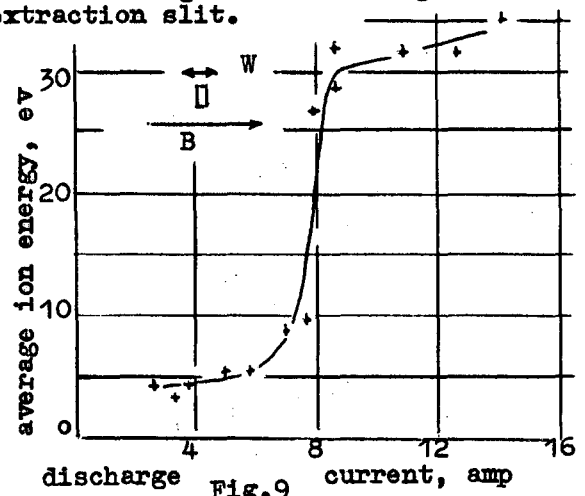

Fig.9

The average transverse ion energy along the magnetic field. Transversal extraction slit.

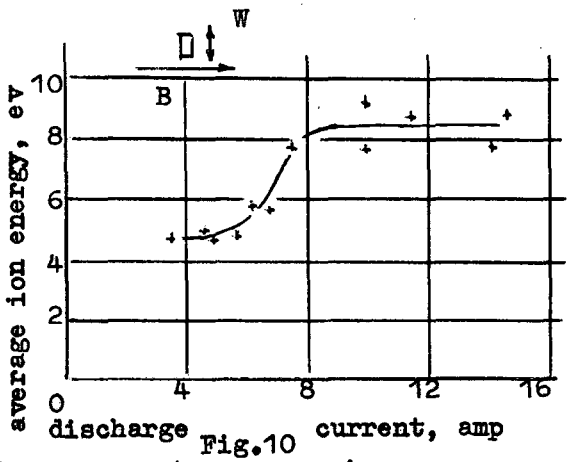

Fig.10

The average transverse ion energy across the magnetic field. Transversal extraction slit.

We can notice the fact that an ion transversal energy dispersedness is always increased when a discharge current becomes greater then 6 - 9 A. First kind oscillations exitation threshold lies in the same region of discharge current values when gas pressure p = 5·10 torr.

Dispersedness across a magnetic field is the same for both slits and consist 4 - 9 ev at lowest and highest levels, correspondently.

As for dispersedness along a field, it rise not strongly for the longitudial slit (40 mm in this direction). It is not surprizing, in spite of structure of oscillations. But for the second slit (2 mm in this direction) dispersedness rises very strongly. As we can see, it approaches 35 - 30 ev. Doubtless, that in this case a boundary conditions are essential.

References

[1] Gabovitch M.D. et al. JTP 30 345 (1960)

[2] Kistemaker J, Sneider J. Physica, 19 950 (1953)

[3] Kadomtsev B.B. Voprosy teorii plasmy ,1964

[4] Hoh F. Phys.Fluids 6 1184 (1963)

[5] Simon A. Phys.fluids 6 382 (1963)

FORMATION OF INTENSE ION BEAM WITH A MULTIPLE-SLOT EXTRACTOR

V.M.Kulygin, A.A.Panassenkov, N.N.Semashko

I.V.Kurchatov Institute of Atomic Energy , Moscow , USSR

V.S.Boldasov, B.I.Volkov, A.G.Sveshnikov

Moscow State University , USSR

Formation of intense beams of energetic hydrogen atoms by charge exchange of ion beams in a gas cell, formed by hydrogen gas flow from an ion source, demands to pay particular attention to design of the source extractor. Experimental selection of extractor geometry demands large spending of time because of the ion beam quality dependence on many extractor and source plasma parameters.

As a preliminary the design of extractor was investigated with the aid of digital computer program, which determines the trajectories of ions from a plasma surface through the extractor taking into account the space charge of the beam. We assume the plasma boundary is hard and electric field does not penetrate into the plasma. Thus, we may consider the plasma boundary as a solid surface on which the potential and the current densities are constant. The effect of plasma temperature is neglected.

The shape and position of the plasma boundary is found from the boundary conditions, subject to the normal electric field vanishing at every point on the plasma surface. This is consistent with the assumption that the emitting plasma surface positions itself in such a way that the ion current density at the emitter is simultaneously emission-limited and space-charge-limited at every point on the surface.

The mathimatical problem consists in solving the system of motion equations

$$m\frac{d^2\vec{r}}{dt^2} = -e\nabla\varphi \qquad (1)$$

and boundary value problem for the potential φ of the total electric field in the domain T

$$\Delta\varphi = -4\pi\rho(M), \quad M \in T \qquad (2)$$

$$\varphi|_{\Gamma_1} = 0, \quad \varphi|_{\Gamma-\Gamma_1} = \varphi_0(P), \quad P \in \Gamma-\Gamma_1$$

where Γ_1 is the plasma surface - the unknown part of the boundary of the domain T, $\Gamma-\Gamma_1$ is the given part of the boundary of the extraction region on which the potential $\varphi_0(P)$ is perscribed.

The shape and position of the unknown boundary Γ_1 is found from the boundary condition

$$\frac{\partial\varphi}{\partial n}\Big|_{\Gamma_1} = 0 \qquad (3)$$

On this boundary the value of the ion current density is given

$$\vec{j}|_{\Gamma_1} = j_0\vec{n} \qquad (4)$$

where $\vec{n}$ is a unit vektor, normal to the surface Γ_1.

To complete the statement of the problem, we must choose the algorithm for the charge density calculation. There are several types of such algorithms. In this report we use the "particle in cell" method. The value of j_0 determines the charge and the frequency of particle emission.

The problem (1) - (4) is solved, using the "particle in cell" method and the relaxation method. For this, the condition (3) is replaced by the condition of the "moving" boundary [1]

$$\frac{ds}{d\tau} = \alpha\frac{\partial\varphi}{\partial n}\Big|_{\Gamma_1} \qquad (5)$$

where s - is the displacement of the boundary in the direction of its normal $\vec{n}$, and α - is some iterative factor.

The boundary value problem (2) for each time step is solved by means of Peaceman - Rachford modification of finite difference method, using the difference schemes of second order approximation.

The major iteration cycles in τ are repeated until the change in the position of the moving boundary Γ_1 becomes within the accurancy criterion. Our aim is to find the optimal configuration of the ion sourse. For the criterion of optimisation the

"angle of divergence" θ is choosen - the angle in which the current density at the output of the system decreases e times.

We consider two configurations of the extractor. The first is given on fig.1. There A - is the beam-forming B and C - accel-deccel electrodes, D - the collector. On lines of symmetry

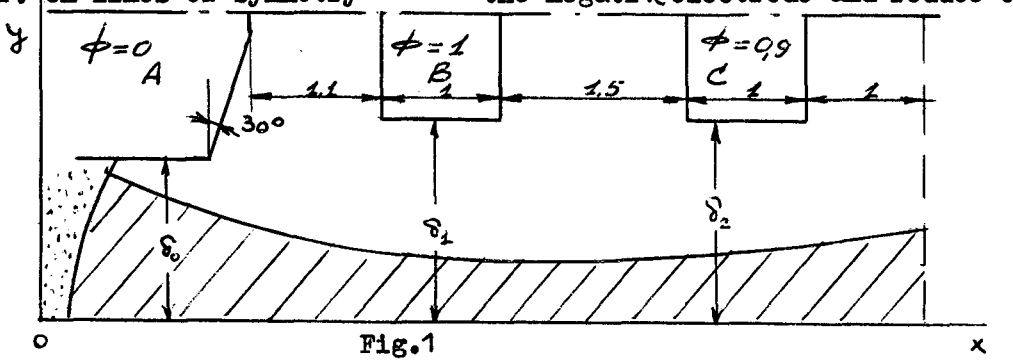

Fig.1

Ion - optic system configuration. All dimentions are normalised by a = 2 mm .

$y = 0$ and $y = y_m$ the following conditions for the potential

$$\left.\frac{\partial \varphi}{\partial n}\right|_{y=0} = 0, \quad \left.\frac{\partial \varphi}{\partial n}\right|_{y=y_m} = 0 \qquad (6)$$

and conditions of mirror reflection for charged particles have to hold.

Fig.2 shows the angle θ as a function of an ion current density at the plasma boundary for various values of the aperture of the beam - forming electrode A . With increasing of the

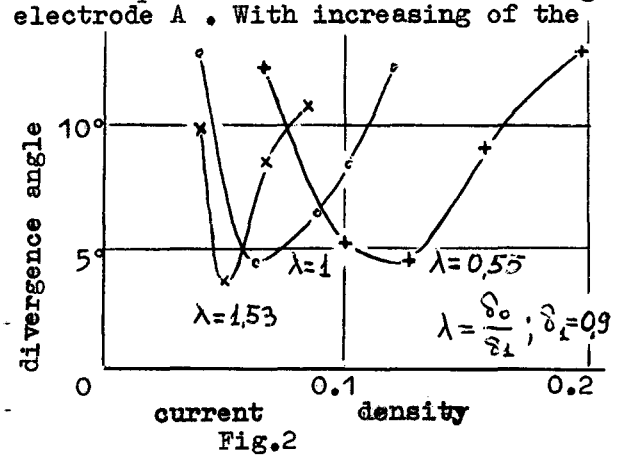

Fig.2

Divergence angle θ as a function of the aperture of the beam-forming electrode A.

aperture, the angle θ slightly decreases. The corresponding curves in a vicinity of extremal points become more and more sharp. It indicates that for this configuration of the extractor the optimal regime is not stable - small current density variations lead to a large change in the angle θ .In fig.3 the angle θ is plotted as a function of the aperture. This result has a particular practical importance: we can enlarge the aperture width of the negative electrode and reduce electrical drain to negative electrode without increasing of a beam divergence.

Our investigations forced us to change the geometry of electrodes of the extractor.New geometry is shown in fig.4. In fig.5 (solid line) the dependence of angle θ on the current density at plasma surface is shown. The avantage of this configuration is in the smaller value of the optical angle θ and in more smooth dependence of θ on variations of the current density.

Extensive numerical calculations results have determined the best configuration of the extractor that we have built and tested. The experiments were made with ion beam, extracted from the source without external magnetic field (like that, described in 1). The beam current density distri-

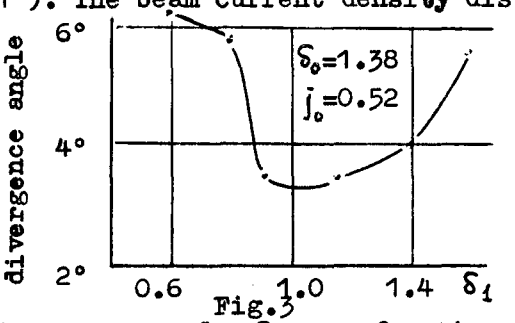

Fig.3

Divergence angle θ as a function of the aperture of accelerating electrode

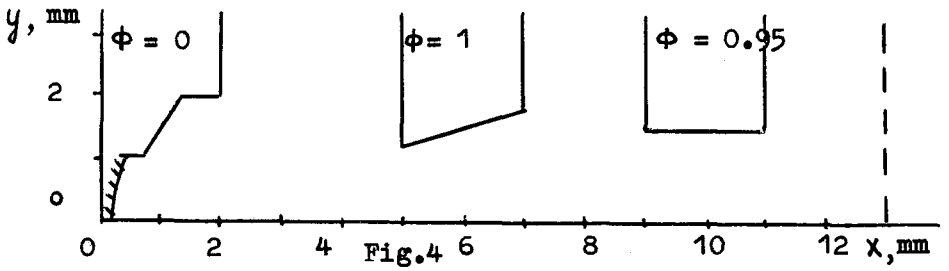

Fig.4 Ion - optic system configuration. The second variant.

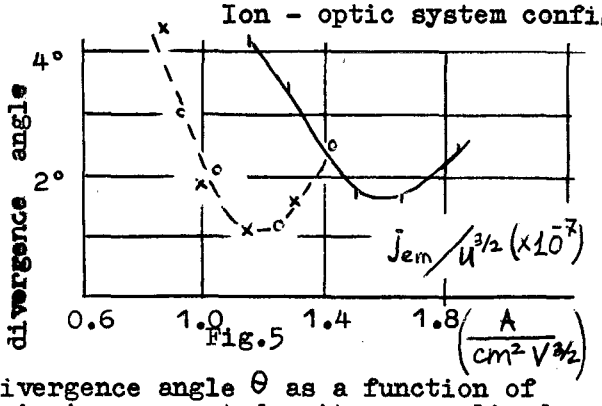

Fig.5 Divergence angle θ as a function of emission current density, normalized on $U^{3/2}$. Solid line - calculation results. Experimental points : (○) - U_0 = 15 KV ; (×) - U_0 = 20 KV

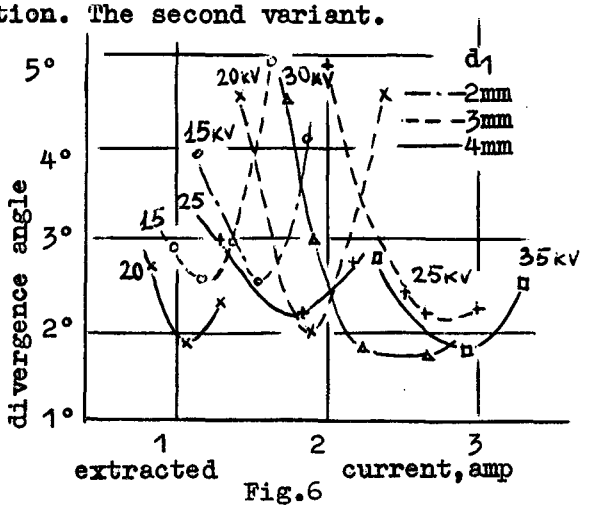

Fig.6 Divergence angle θ as a function of emission current for various accelerating voltages and values of accelerating gap (d_1).

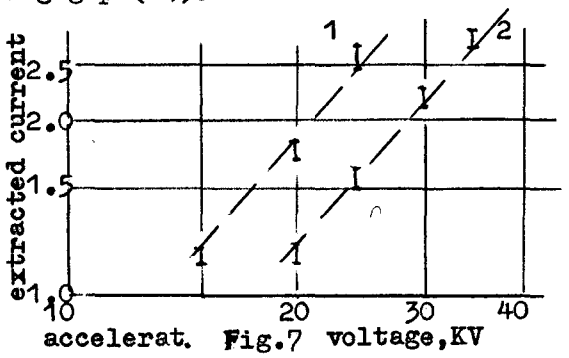

Fig.7 Optimum beam current as a function of accelerating voltage. 1 - d_1=3 mm ; 2 - d_1=4 mm .

bution was measured at the distance 1.3 m from the source. As a preliminary, a single-slot extractor of the same design as shown in fig.4 has been tested. Fig.5 (dashed line) shows beam divergence angle (1/e half-width) perpendicular to the slot as a function of an ion emission current density(j_+) One can see that character of the dependence is similar to the calculated one, divergence angle is slightly less but the optimum value of j_+ is 1.4 times less than calculated ones. The measured angle of the beam divergence in the plane of the slot was less than 1° and wasn't practically dependent on beam current.

Intense ion beam extraction and forming was made with the aid of nine-slot extractor with the total emission area 9.5 cm^2. Beam divergence perpendicular to the slots was measured with beam current change for different values of accelerating gap (2 ÷ 4 mm) and voltage (15 ÷ 35 KV). The results of measurements are shown in figs. 6 and 7 . One can see the fact that minimum values of beam divergence angle are approximately the same in spite of rather wide range of parameter changes. That means that plasma boundary optimum form is approximately the same in all cases. However, it turns out that values of minimum θ are more and values of optimum j_+ are less in the case of nine-slot extractor than for singl-slot extractor. This discrepancy is connected with nonuniformity of the ion sourse discharge plasma near the emission surface and, therefore, with unequal conditions of working of different slots. Fig.7 shows that when plasma boundary has optimum position (minimum of θ) the extracted beam current is proportional to 3/2 power of

extracting voltage.

References

[1] Boldasov V.S. et al. Dokl. Ac.Nauk 201 (1971)
[2] Berkner K.H. et al. CN-28/G-11 Conference on plasma physics and controlled fusion. Madison, june 1971

INVESTIGATION OF A GAS CELL PLASMA, GENERATED BY CHARGE EXCHANGE OF INTENSE ION BEAM

V.M.Kulygin , A.A.Panassenkov
I.V.Kurchatov Institute of Atomic Energy
Moscow , USSR

Abstract

The parameters of a secondary plasma, generated in a gas cell by charge exchange of hydrogen ion beam, extracted from a plasma source, are investigated. Measurements show that secondary plasma parameters change considerably along the gas cell. Near the source plasma density is about $5\cdot10^{10}$ cm^{-3}, electron temperature is about 1 eV, plasma potential is about 4 V. To the end of the cell plasma density decreases considerably, electron temperature increases to 7 ÷ 8 eV, plasma potential increases to 60 V.

Intense beams of energetic hydrogen atoms are usually produced by charge exchange of ion beams in a gas cell. Charge exchange and ionization collisions of ions with gas atoms lead to generation of a secondary plasma, which density can be much more the density of the incident beam. This cold plasma can influence on the characteristics of passing ion and produced atom beams.

In this paper we describe the measurements of parameters of the secondary plasma, generated by charge exchange of hydrogen ion beam (beam current up to 2 A, energy 15 ÷ 30 keV), extracted from a plasma source without external magnetic field, similar to the source, described in [1]. Neutralization of the ion beam is accomplished by electron capture collisions in hydrogen gas, flowing from the source through a duct 80 cm long. Gas pressure has maximum adjacent to the ion source and decreases to the end of the duct. Measurements of the secondary plasma parameters were made with the aid of three plane probes, placed near the duct wall at the distances 14, 42 and 68 cm from the ion source extractor.

As a preliminary, let us estimate the secondary ion current density distribution on the duct wall, when there is a flow of energetic protons and neutrals through a gas cell. The rate of the secondary ions generation per volume unit is

$$\frac{dn_+}{dt} = n_0 v_1 \left[\sigma_1 n_1 + \sigma_0 \bar{n}_0\right], \qquad (1)$$

where n_0 is the hydrogen molecules density, v_1, n_1 and $\bar{n}_0$ are the velocity and densities of energetic protons and neutrals, σ_1 and σ_0 are the summarized cross-section for production of the secondary ions (mainly H_2^+ ions) by protons and neutrals in hydrogen gas. Values of n_0, n_1 and $\bar{n}_0$ are the function of the distance from the source (z-coordinate). Let us assume the secondary ions go out of the cell volume in radial direction to the duct wall. Integration of (1) over r allows to ob-

tain the secondary ions current density to the duct wall:

$$j_+ = \frac{I_i}{2\pi R} n_o \left[\sigma_1 \Phi_1 + \sigma_o \Phi_o\right], \qquad (2)$$

where I_i is the ion beam current, R is the duct radius, Φ_1 and Φ_o are dependent on z fraction of energetic protons and neutrals, $\Phi_1 + \Phi_o = 1$. If the gas flow through the duct is molecular, the pressure gradient will be linear

$$n_o(z) = n_{oo}(1 - z/L),$$

where n_{oo} is adjacent to the source density of hydrogen molecules. Gas pressure out of the duct ($z > L = 100$ cm) is practically zero. In this case one can receive the expressions for dependence of Φ_1 and Φ_o on z:

$$\Phi_1 = \frac{\sigma_{01}}{\sigma_{10}+\sigma_{01}} + \frac{\sigma_{10}}{\sigma_{10}+\sigma_{01}} \exp\left[-n_{oo}(\sigma_{10}+\sigma_{01}) z \left(1 - \frac{z}{2L}\right)\right]$$

$$\Phi_o = \frac{\sigma_{10}}{\sigma_{10}+\sigma_{01}} \left\{1 - \exp\left[-n_{oo}(\sigma_{10}+\sigma_{01}) z \left(1 - \frac{z}{2L}\right)\right]\right\} \qquad (3)$$

where σ_{10} and σ_{01} are cross-sections for electron capture and reionization.

Using expressions (2) and (3) we have calculated the dependence of j_+ on z for different neutralizer thicknesses $\pi_i = 0{,}5\, n_{oo} L$ and beam energy range 15 ÷ 30 keV. Probes measurements allowed to obtain the distribution of j_+, electron temperature (T_e), and plasma potential (φ_{pl}) along the beam line for different beam currents and energies. Evaluation of experimental neutralizer thickness according to the gas flow from the source and conductance of neutralizer duct gave value of π_i in the range of $(0{,}6 \div 1{,}2)\cdot 10^{16}$ cm^{-2}. Experimental values of j_+ at the different distances from the source agree well with calculated ones for $\pi_i = 1\cdot 10^{16}$ cm^{-2} (fig.1). One can see fairly

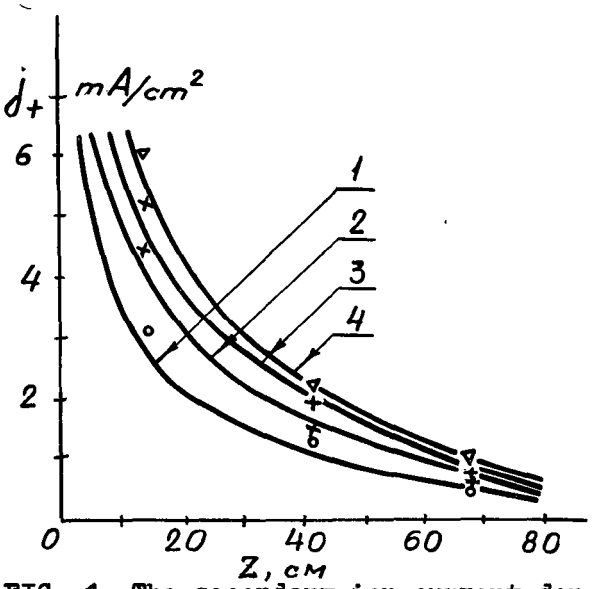

FIG. 1. The secondary ion current density to the duct wall as a function of the distance from the source. Solid lines are the results of calculations for the target thickness $1\cdot 10^{16}$ cm^{-2} and beam energies and currents, correspondingly: 1) 15 kV, 1,1 A 2) 20 kV, 1,6 A 3) 25 kV, 1,8 A 4) 30 kV, 2 A.

rapid decreasing of j_+ along z and increasing of T_e and φ_{pl} (fig.2). Secondary plasma density reaches $\sim 10^{11}$ cm^{-3} near the ion source and decreases more rapidly than j_+.

Measurements show that increasing of electron temperature with the distance from the source does not strongly depend on beam current and energy. It is known [2] that secondary electrons, resulting from ionization of hydrogen gas by energetic protons, have velocities mainly along the primary proton beam, so the increasing of T_e along the beam path can be explaned by some scattering mechanism. But the mean free path of electrons is longer then the duct length. To all appearance it is possible to explain this effect by means of some collective mechanism,

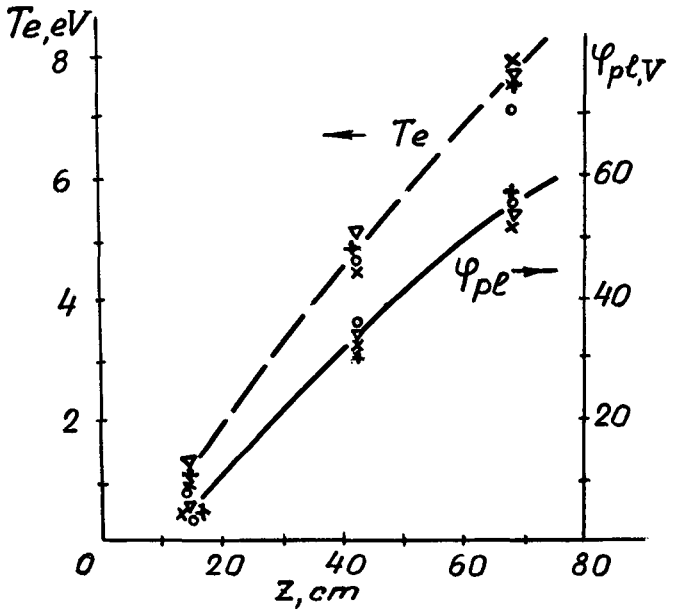

FIG. 2. The electron temperature and potential of secondary plasma as a function of the distance from the source. (∘) - 15 kV, (×) - 20 kV, (+) - 25 kV, (▽) - 30 kV.

but we have no sufficient data now.

References

1. K.H.Berkner et al. Paper CN-28/G-11 IV Conf. on Plasma Phys. and Control. Nucl. Fusion Research, Madison (1971).
2. C.E.Kuyatt, T.Jorgensen,Jr. Phys. Rev. 130, 1444 (1963).

THE ION SOURCE WITH RADIAL DISCHARGE IN THE CUSP MAGNETIC FIELD

N.N.Semashko, N.V.Pleshivtsev, V.V.Kuznetsov, B.P.Maximenko, N.P.Malakhov

I.V.KURCHATOV INSTITUTE OF ATOMIC ENERGY, MOSCOW, USSR

Abstract

The ion source with the large emission surface designed to obtain intensive beams of hydrogen ions with the current intensity of tens of amperes for injectors of fusion installations, is discribed. The source is placed in the cusp magnetic field. A discharge is ignited nearly the median surface of the field along the magnetic force line over the radius between the cylindrical cathode and external anode located coaxially, forming the plasma ring. Its lateral surface serves as an ion emitter. The ion concentration in the plasma with the large emission surface doesn't decrease with the increase of radius of emission ring slits, since the magnetic field strength increases over the radius. Ions are extracted from the plasma across the magnetic force lines and accelerated by means of three-electrodes electrostatic system along the longitudinal axes of solenoids, generating the cusp magnetic field. Experiments were carried out with one and two ring slits of emission with width 2 mm and mean diametr 130 and 160 mm. The discharge current reached 500 A. The average density of emission current of ions amounted to 0,8 A/sm^2. The current in beam of ions under 40 keV exceeded 16 A.

Introduction

At the present time, much attention of CTR program is being given to experiments with the external injection of fast particles in magnetic traps. Requirements of experiments with the high-temperature plasma set a task to develop powerful injectors providing generation of ion beams and fast atoms fluxes of hundreds of amperes and of energy to 100 keV.

As it is known, in plasma ion sources the generation of intensive focused beams of ions is limition by the effect of space charge, electric strength of accelerating gap and some difficulties in generating the gas-discharge plasma having a stable emission surface with high and uniform concentration of ions. Under real condition these factors do not allow ion flows to be obtained with the current density over 1 A/cm^2. Therefore, one of obvious possibilities to increase essentially the beam current is a considerable expansion of plasma emmision surface from which ions are extracted.

Scheme of ion source

The ion source "MIR" with a radial discharge and ring emission slits placed in the cusp magnetic field which is set up by two solenoids mounted on a single axis and connected in opposition (FIG.1) meet the requirements mentioned above. In proximity to the median surface of the magnetic field along lines of force over the radius the arc discharge is ignited, forming a plasma disk. Ion are extracted out of the gas-discharge chamber across lines of magnetic force and accelerated by means of electrostatic system with ring slits. The area near the axis of magnetic field is eliminated from the space occupied by the discharge. Since the magnetic field strength nearly the median surface tends to zero when approaching

the longitudinal axis, therefore, the discharge is set up starting from some radius (the radius of cathode) which value is determined by the stability of discharge ignition in a weak magnetic field. At the external side the discharge is limited by a radius being equal approximately to 2/3 of the inner radius of coil the magnetic field. Almost the whole of the plasma surface nearly the median surface can be used for extraction of ions. therefore, several ring emission slits can be aligned here concentrically.

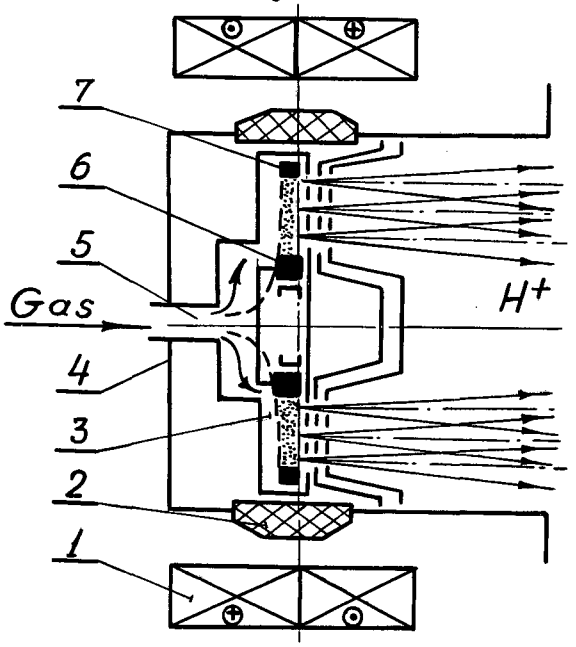

FIG. 1. Principal scheme of the ion source with radial discharge. 1-solenoids, connected in opposition, 2-high-voltage insulator, 3-discharge chamber, 4-case of the source, 5- gas-distributor, 6-heated cathode, 7-anti-cathode, 8-accelerating electrode, 9-grounded electrode.

Because the magnetic field strength increases over the radius, the plasma concentration will not be diminished with the increase of radius as a consequence of wich the total current of ions will grow proportional to the total overall length of all emission slits.

At the output from the source magnetic field the azimuthal component of velocity is absent at the beam owing to position of the emission surface nearly the median surface, where the longitudial component of the field is missing.

At the given source design "MIR-3" working at the voltage 20-40 kV the area of one emission slit is about 10 cm^2; when use is made of five ring slits and the current density of ions 1 A/cm^2, one can produce from this ion source the beam with the current to 50A.

In the source walls of its gas-discharge chamber are anode of arc discharge and the positive pole of acceleration system. The discharge chamber has the 10 mm height and 200 mm outer diameter. It is limited by the ring cathode over the 50 mm inner radius. Close to the external wall where is a ring insulated from the case, which can serve as an anti-cathode or anode. 12 probes serving for investigation of plasma parameters, are uniformly placed over the circle on this ring. A gas is supplied in the gas-discharge chamber by pulses through the ring slit having the 0,1 mm width in such a manner that the gas curtain is created above the cathode surface and the straight flow of gas into emission slits is not occured. A pressure in the gas-discharge chamber in the course of arc ignition was 10^{-3} - 10^{-2} mm Hg.

The cathode unit consists of a heated cathode in the shape of a ring of 100 mm diameter made of LaB_6 and the ring of tantalum ribbon. The internal surface of cathode and the heater are separated from the dischatge chamber and placed in vacuum. The cathode is heated to emission temerature by the radiation and by the electron bombardment. Electrons are accelerated to the energy of 0,5-1,0 keV.

A system of beam extraction and acceleration comprises three electrodes which accelerate ions and slow down the electron flow generating by the ion beam. Ions are extracted from the arc discharge plasma through the concentric ring slips of the 2-4 mm width. When operating without an accelerating voltage the probes which served for measurins the azimuthal and radial characteristics of radial arc discharge, were inserted into the emission slits.

Experimental results

One of the most important and insufficiently investigated problem is stability of discharge and its azimuthal and radial homogenity. First experiments on the discharge investigation and extraction of the ion beam have shown a considerable azimuthal inhomogenity of in distribution of the

discharge current and the beam current over the azimuth (FIG.2).

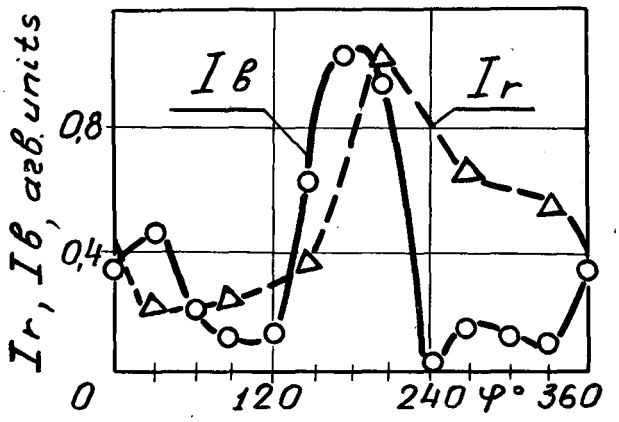

FIG.2.Azimutal distribution of the discharge current (I_r) and beam current of hydrogen ions (I_b).

This azimutal inhomogeneity was largely by the non-uniform heating of the ring cathode.The azimuthal inhomogeneity was essentially decreased when the cathode unit with movabl holders of the heater had been made.They allowed the distance between the cathode and the heated filament to be changed in the course of operation of the source. Fig.3 presents the azimuthal distribution of signals of slit probes measured with the three-slit emission lens.

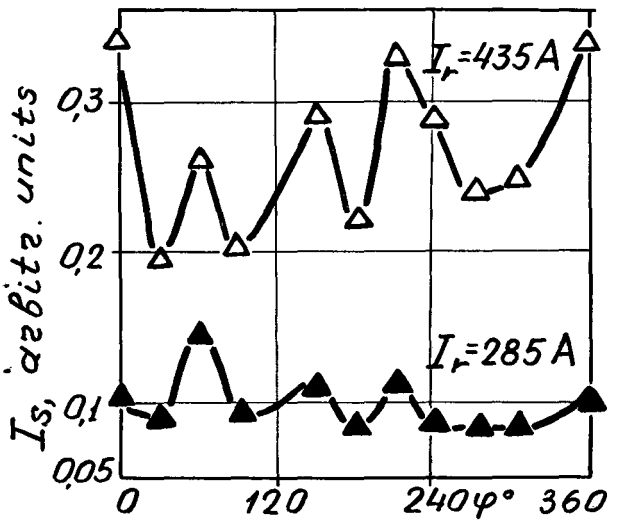

FIG.3.Azimuthal distribution of currents on slit probes at discharge cuurrents 285 and 435 A.

For the lower curve measured at the discharge current of 285 A the maximum deviation of probe signals from the mean value did not exceed 15%.With the increase of discharge current this deviation has increased and at the discharge current of 435 A it has reached 30%.Further decrease in inhomogeneity of the discharge requires improvements in design of the given cathode unit.

To investigate a behavior of the discharge in the radial direction the five-slit emission lens was mounted on the discharge chamber,and five slit probes,positioned on radii 63,72,81,90 and 99 mm,were mounted in one of azimuths of this lens.The width of slits was 2 mm.Fig.4 shows a distribution of probe signals:.

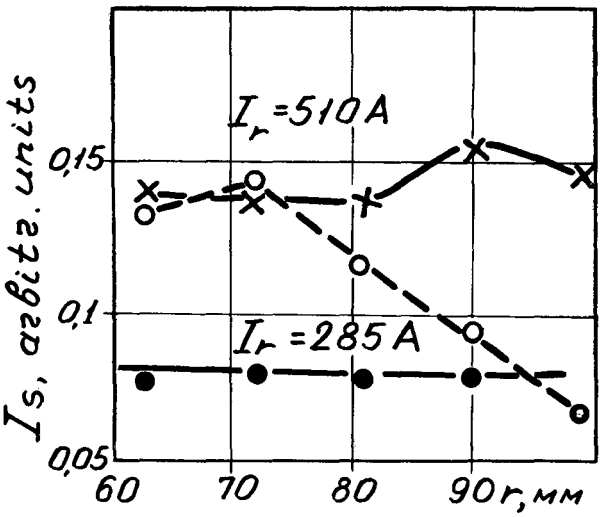

FIG.4.Radial distribution of currents on slit probes at discharge currents of 285 and 510 A.Solid lines-the median surface of magnetic field coincides with the symmetry plane of gas-discharge chamber;dotted lines-the median surface is displaced by 2 mm from the symmetry plane.

It is shown that when the median surface of the magnetic field is coincided with the symmetry plane of the discharge chamber (by displacement of coils),the radially uniform distribution of ion current on probes is set up.A uniformity of distribution is disturbed on large radii already at the small displacement of median surface from this optimum position.These measurements show that the discharge is rather strongly magnetized and "rigidly"bound with lines of magnetic field.Estimates carried out with the probe measurement

give the current density of ion emission within the limits of 0,5-0,8 A/cm^2.

Experiments on the extraction of ion beam were carried out with the single-slit and two-slit ion optics. In the case of single-slit optics use was made of the following geometry of accelerating gap: the mean radius of circle of the emission slit amounted to 75 mm at the slit width of 2 mm;the width of slit in the accelerating electrode was 4 mm;the width of slit in the grounded electrode was 10 mm; the length of accelerating and deccelerating gaps were equal to 2 and 8 mm,respectively.Dimensions of the ion-optics system were calculated for experiments with beams of hydrogen ions with the energy from 20 to 40 keV.Geometry of two-slit optics was somewhat different from single-slit one.

To determine the current of accelerated ions the total load current of high-voltage supply system was measured,which involves the sum of the beam current at the exit of the ion-optic system,the beam current reaching the accelerating electrode,and the current of high-voltage PIG discharge developing around the ion source.Besides,the current of accelerated ions was intercepted by the movable target which provided both the electric and calorimetric measurements of ion current. The ion current on the accelerating electrode turned out to be compared with the current of high-voltage discharge and was within the limits of 0,1 A.

In the course of experiments the optimization of operating conditions of the source over the value of gas supply,the discharge current,the magnetic field,the voltage on the deccelerating electrode,and the working conditions of the cathode unit and the position of the median surface relative to emission slit were optimized as well.

From total experimental data obtainid from both single-slit and the two-slit optics presented in fig.5,it is seen that the extracted ion current increases with the growth of the disctarge current and the accelerating voltage.At the comparable conditions of arc firing but not optimized other parameters,the beam current from the two-slit lens has increased to the average 1,5 times as compared with one-slit ion optics.The maximum value of current for accelerated ions in the beam reched 20 A at the energies of hydrogen ions 30-40 keV.The divergence angle of the beam was within the limits of $\pm 5°$ in this case.

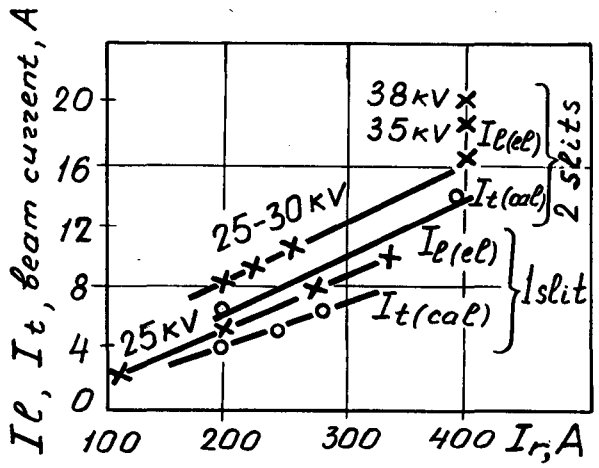

FIG.5.Depedence of total current of accelerated beam and current of ions on the target on the distharge current for single-and two-slit ion optics.

Conclusion

Thus,the design of the ion source with the radial discharge in the cusp magnetic field permitting to generate the gas-discharge plasma with the high emission surface (400 cm^2 and over), featuring the high emissive power (o,8 A/cm^2) was offered and practically realized.The beam of hydrogen ions with the current of 20 A was obteined,the works on generating the beam with the current of 50 A and energy to 100 keV are being carried out.